

Chapter 16

Electronic Spectroscopy of Diatomic Molecules

P.F. Bernath

University of Waterloo, Waterloo, Ontario

1 Introduction	3
2 Born–Oppenheimer Approximation	3
3 Separation of Vibration and Rotation	4
4 Electron Spin and Nuclear Spin	5
5 Notation	5
6 Franck–Condon Principle	7
7 Rotational Line Strengths	8
8 Spectroscopic Constants and Potential Energy Curves From Ab Initio Calculations	8
9 Calculation of Relativistic Effects	11
10 Calculation of Lifetimes and Transition Dipole Moments	12
11 Calculation of Bond Energies, Ionization Potentials, and Electron Affinities	13
12 Conclusion	14
Note	14
References	14

1 INTRODUCTION

The study of the electronic spectra of diatomics has a long history. Prominent diatomic spectra include the green color of the Swan system of C_2 that can be seen in a Bunsen burner flame,⁽¹⁾ the emission of N_2 in the aurora⁽²⁾ and the atmospheric A-band absorption of oxygen first seen by Fraunhofer.⁽³⁾ The spectra of TiO were seen in

Handbook of Molecular Physics and Quantum Chemistry, Edited by Stephen Wilson. Volume 3: *Molecules in the Physicochemical Environment: Spectroscopy, Dynamics and Bulk Properties*. © 2002 John Wiley & Sons, Ltd

stars⁽⁴⁾ well before any interpretation of the bands could be made. The development of quantum mechanics and the Born–Oppenheimer approximation⁽⁵⁾ led to the quantitative understanding of electronic spectra.

In this chapter, we begin with a discussion of the basic principles of the electronic spectroscopy of diatomic molecules.^(6,7) The rest of the chapter is devoted to a discussion of the ab initio calculation of molecular properties associated with the electronic spectra of diatomic molecules. The calculated properties will be compared with experimental observations for selected examples.

2 BORN–OPPENHEIMER APPROXIMATION

The interpretation of the electronic spectra of diatomic molecules begins with the nonrelativistic Hamiltonian in the laboratory coordinate system, namely,

$$\hat{H} = -\frac{\hbar^2}{2m_A}\nabla_A^2 - \frac{\hbar^2}{2m_B}\nabla_B^2 - \frac{\hbar^2}{2m_e}\sum_{i=1}^N\nabla_i^2 + \hat{V} \quad (1)$$

for the usual electrostatic potential \hat{V} , nuclei A, B with masses m_A , m_B and N electrons of mass m_e . Transforming to the nuclear center-of-mass relative coordinate system and removing the center-of-mass kinetic energy⁽⁸⁾ results in the new Hamiltonian,

$$\hat{H} = -\frac{\hbar^2}{2\mu}\nabla_r^2 - \frac{\hbar^2}{2m_e}\sum_{i=1}^N\nabla_i^2 - \frac{\hbar^2}{2(m_A + m_B)} \times \sum_{i,j}^N\nabla_i\cdot\nabla_j + \hat{V} \quad (2)$$

with

$$\mu = \frac{m_A m_B}{m_A + m_B} \quad (3)$$

being the reduced mass of the two nuclei, and \mathbf{r} the vector from nucleus A to nucleus B. The third term on the right-hand side of equation (2) is the ‘mass-polarization’ term that has appeared because of the transformation from laboratory to nuclear center-of-mass coordinates. The mass-polarization term is generally neglected because it makes a small contribution to the energy. Other choices of internal coordinate systems are possible⁽⁸⁾ [1] and then the mass-polarization term in equation (2) takes on a different form.

The next step is the separation of electronic and nuclear motion through the Born–Oppenheimer approximation. The wave functions $[\psi_n(\mathbf{r}_i; \mathbf{r}), n = 1, 2, \dots]$, solutions of the electronic Schrödinger equation

$$\hat{\mathbf{H}}_e \psi_n(\mathbf{r}_i; \mathbf{r}) = U_n(\mathbf{r}) \psi_n(\mathbf{r}_i; \mathbf{r}) \quad (4)$$

with

$$\hat{\mathbf{H}}_e = -\frac{\hbar^2}{2m_e} \sum_{i=1}^N \nabla_i^2 + \hat{V} \quad (5)$$

form a complete set. The electronic Schrödinger equation is solved for the N electrons as a function of \mathbf{r}_i at a particular value of \mathbf{r} , the relative internuclear coordinate. The resulting wave functions, labeled by the index n , with the energy eigenvalues $U_n(\mathbf{r})$ are parametric functions of \mathbf{r} . The $U_n(\mathbf{r})$ generate the usual potential energy curves for the states.

The wave functions needed to solve equation (2) are written in the form

$$\psi = \sum_j \psi_j(\mathbf{r}_i; \mathbf{r}) \chi_j(\mathbf{r}) \quad (6)$$

so that after premultiplying by ψ_k^* and integrating over the electronic coordinates, the differential equation

$$-\frac{\hbar^2}{2\mu} \nabla_r^2 \chi_k + [U_k + H'_{kk} - E] \chi_k = - \sum_{j \neq k} H'_{kj} \chi_j \quad (7)$$

appears, in which the H'_{kk} are the diagonal matrix elements of the mass-polarization operator as well as of some additional derivatives with respect to nuclear coordinates from the r -dependence of the electronic wave functions. Because the set of coupled differential equation (7) is difficult to solve, further approximations need to be made.

In the ‘clamped-nuclei’ approximation, both the nondiagonal terms (H'_{kj}) on the right-hand side of equation (7) and the diagonal correction (H'_{kk}) are neglected to yield the

simple equation

$$-\frac{\hbar^2}{2\mu} \nabla_r^2 \chi_k + U_k \chi_k = E \chi_k \quad (8)$$

for nuclear motion within the k th electronic state on the potential energy surface. The effects of mass polarization and the Born–Oppenheimer approximation can be accounted for by using perturbation theory to correct for the neglected diagonal (H'_{kk}) and off-diagonal (H'_{kj}) terms in equation (7).

3 SEPARATION OF VIBRATION AND ROTATION

Equation (8) for nuclear motion accounts for the vibrational and rotational motion of a diatomic molecule [1]. For $^1\Sigma^+$ states, the separation of vibration and rotation is simple, because the square of the gradient operator for the relative coordinates can be written as

$$\nabla_r^2 = \frac{\partial^2}{\partial r^2} + \frac{2}{r} \frac{\partial}{\partial r} - \frac{1}{\hbar^2 r^2} \hat{\mathbf{J}}^2 \quad (9)$$

in which $\hat{\mathbf{J}}^2$ is the square of the rotational angular momentum operator,

$$\hat{\mathbf{J}}^2 = -\hbar^2 \left(\frac{\partial^2}{\partial \theta^2} + \cot \theta \frac{\partial}{\partial \theta} + \frac{1}{\sin^2 \theta} \frac{\partial^2}{\partial \phi^2} \right) \quad (10)$$

The $\hat{\mathbf{J}}^2$ operator commutes with the Hamiltonian operator in equation (8) and has the governing equation

$$\hat{\mathbf{J}}^2 Y_{JM}(\theta, \phi) = J(J+1) \hbar^2 Y_{JM}(\theta, \phi) \quad (11)$$

in which the $Y_{JM}(\theta, \phi)$ functions are the spherical harmonics. The variables θ and ϕ are the polar and azimuthal angles that define the orientation of the internuclear axis with respect to the laboratory coordinate system. The nuclear motion equation (8) is exactly separable, with

$$\chi(r) = S(r) \frac{Y_{JM}(\theta, \phi)}{r} \quad (12)$$

The resulting differential equation for radial motion (vibration of the nuclei) is

$$-\frac{\hbar^2}{2\mu} \frac{d^2 S}{dr^2} + \left[U(r) + \frac{J(J+1)\hbar^2}{2\mu r^2} \right] S = E S \quad (13)$$

with the centrifugal potential

$$U_{\text{cent}}(r) = \frac{J(J+1)\hbar^2}{2\mu r^2} \quad (14)$$

added to the rotationless potential $U(r)$ for a particular electronic state. Note that although the reduced mass was defined earlier (equation 3) using nuclear masses, it is customary to use atomic masses when computing μ .

The solution of equation (13) for the vibration–rotation energy levels requires a particular potential energy function U . Given U , equation (13) can be solved numerically. Unfortunately, the electronic states of real molecules are not represented by any known analytical potential functions, although many ingenious approximate functions⁽⁹⁾ have been created. A power series expansion, however, can represent any potential on a given interval to arbitrary precision. The customary potential function, due to Dunham,⁽¹⁰⁾ is

$$U(\xi) = a_0\xi(1 + a_1\xi + a_2\xi^2 + \dots) \quad (15)$$

in which $\xi = (r - r_e)/r_e$. Dunham⁽¹⁰⁾ solved equation (13) with potential (15) using the semiclassical quantization condition,⁽⁷⁾ and generated the double power series expression

$$E_{vJ} = \sum Y_{ij} \left(v + \frac{1}{2}\right)^i [J(J+1)]^j \quad (16)$$

for the vibration–rotation energy levels for a $^1\Sigma^+$ electronic state.

The Dunham expression for the vibration–rotation energy levels is equivalent to the usual Herzberg⁽⁶⁾ energy level expressions,

$$G(v) = \omega_e \left(v + \frac{1}{2}\right) - \omega_e x_e \left(v + \frac{1}{2}\right)^2 + \omega_e y_e \left(v + \frac{1}{2}\right)^3 + \dots \quad (17)$$

$$F_v(J) = B_v J(J+1) - D_v [J(J+1)]^2 + H_v [J(J+1)]^3 + \dots \quad (18)$$

$$B_v = B_e - \alpha_e \left(v + \frac{1}{2}\right) + \gamma_e \left(v + \frac{1}{2}\right)^2 + \dots \quad (19)$$

$$D_v = D_e + \beta_e \left(v + \frac{1}{2}\right) + \dots \quad (20)$$

by making the correspondences $Y_{01} = B_e$, $Y_{10} = \omega_e$, $Y_{11} = -\alpha_e$, and so forth.

For a $^1\Sigma^+$ state, labeled by n , the total energy for a given rovibronic state $|nvJ\rangle$ is given by

$$E_{nvJ} = T_e(n) + G(v) + F_v(J) \quad (21)$$

$$E_{nvJ} = T_e(n) + \sum Y_{ij} \left(v + \frac{1}{2}\right)^i [J(J+1)]^j \quad (22)$$

The energy level expression for the general singlet case ($^1\Lambda$) requires only the addition of Λ -doubling to account for the small splitting of the double orbital degeneracy.⁽⁶⁾ The nonsinglet case is considerably more complicated, however,

and the specialized literature needs to be consulted for the energy levels of the general $^{2S+1}\Lambda$ state.^(7,11)

4 ELECTRON SPIN AND NUCLEAR SPIN

The nonrelativistic Schrödinger equation is also not complete,⁽¹²⁾ and additional terms need to be added to equation (1) and therefore will also appear in equations (5) and (8). The largest additional term is needed to account for the presence of electron spin, $\hat{\mathbf{H}}_{\text{es}}$. This term includes spin–orbit coupling (electron spin interacting with the magnetic fields created by electron motion), spin–rotation coupling (electron spin interacting with the magnetic fields created by nuclear motion), and spin–spin coupling (interaction of the magnetic moments of different electrons), namely,

$$\hat{\mathbf{H}}_{\text{es}} = \hat{\mathbf{H}}_{\text{so}} + \hat{\mathbf{H}}_{\text{sr}} + \hat{\mathbf{H}}_{\text{ss}} \quad (23)$$

The effects of $\hat{\mathbf{H}}_{\text{es}}$, sometimes called *fine structure*, are present in nonsinglet states.

A much smaller additional term is needed to account for the effects of nuclear magnetic and electric moments, $\hat{\mathbf{H}}_{\text{hfs}}$, and is called *hyperfine structure*. A nuclear magnetic moment can interact with the other magnetic moments in a molecule (i.e., interaction with electron spins and their orbital motion as well as with other nuclear spins and their nuclear motions). All nuclei with $I \geq 1$ have electric quadrupole moments (because of nonspherical nuclear charge distributions) that can be oriented by the electric field gradients present in molecules leading to nuclear quadrupole hyperfine structure. Thus, the hyperfine coupling Hamiltonian consists of two parts and can be written as

$$\hat{\mathbf{H}}_{\text{hfs}} = \hat{\mathbf{H}}_{\text{ns}} + \hat{\mathbf{H}}_{\text{quad}} \quad (24)$$

in which $\hat{\mathbf{H}}_{\text{ns}}$ is the nuclear spin magnetic moment part and $\hat{\mathbf{H}}_{\text{quad}}$ is the quadrupolar moment part of the hyperfine Hamiltonian.

5 NOTATION

The notation for electronic states of diatomic molecules⁽⁷⁾ parallels that for atoms, with $^{2S+1}\Lambda_\Omega$ used in place of $^{2S+1}L_J$ and

$$\Lambda = \sum_{i=1}^N \lambda_i \quad (25)$$

$$\mathbf{S} = \sum_{i=1}^N \mathbf{s}_i \quad (26)$$

in which λ_i is the projection of the i th electronic orbital angular momentum ℓ_i onto the internuclear axis. Notice that

$$\mathbf{L} = \sum_{i=1}^N \ell_i \quad (27)$$

is no longer a constant of the motion, and that this equation has been replaced by equation (25). Only the projection $\Lambda\hbar$ of \mathbf{L} along the internuclear axis is quantized (when spin-orbit coupling is small).

For a diatomic molecule, the total angular momentum (exclusive of nuclear spin) is the vector sum of orbital (\mathbf{L}), spin (\mathbf{S}), and rotational (\mathbf{R}) angular momenta, $\mathbf{J} = \mathbf{L} + \mathbf{S} + \mathbf{R}$ (Figure 1). The total angular momentum \mathbf{J} has a projection of $\Omega\hbar$ units of angular momentum along the molecular axis and (as always) M_J along the space fixed Z -axis (Figure 2). The various angular momenta and their projections onto the molecular axis are summarized in Table 1. The Ω quantum number is sometimes appended as a subscript to label a particular spin component.

For $\Lambda > 0$, there is a double orbital degeneracy corresponding to the circulation of the electrons in a clockwise or counterclockwise direction. This degeneracy remains for $\Omega > 0$, and it is customary to use $|\Omega|$ to represent both values. For example, a ${}^2\Pi$ state has ${}^2\Pi_{3/2}$ and ${}^2\Pi_{1/2}$ ($\Lambda = 1$, $\Sigma = \pm 1/2$) spin components. Notice that there are always $2S + 1$ spin components, labeled by their $|\Omega|$ values except when $S > |\Lambda| > 0$. In that case, there is a notational problem in labeling the $2S + 1$ spin components, so $\Omega = |\Lambda| + \Sigma$ is used instead of $|\Omega|$. For example, for a ${}^4\Pi$ state ($S = 3/2$, $\Lambda = 1$) the spin components are labeled as ${}^4\Pi_{5/2}$, ${}^4\Pi_{3/2}$, ${}^4\Pi_{1/2}$, and ${}^4\Pi_{-1/2}$. The electronic states of diatomic molecules are also labeled with letters: X is

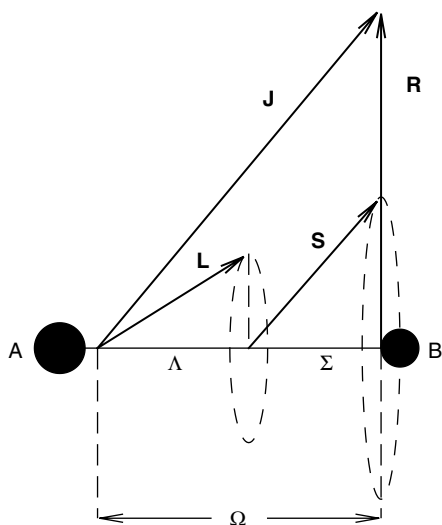


Figure 1. Angular momenta in a diatomic molecule.

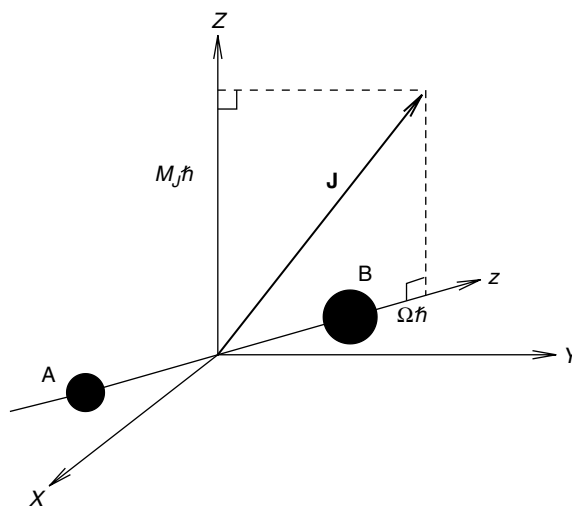


Figure 2. Components of the total angular momentum \mathbf{J} (exclusive of nuclear spin) in the laboratory (X, Y, Z) and molecular (x, y, z) coordinate systems.

reserved for the ground state, while A, B, C , and so on, are used for excited states of the same multiplicity ($2S + 1$) as the ground state, in order of increasing energy. States with a multiplicity different from that of the ground state are labeled with lowercase letters a, b, c , and so on, in order of increasing energy. This convention is illustrated by the energy level diagram of the low-lying electronic states of O_2 in Figure 3. An alternate convention widely adopted by the quantum chemistry community is to label states of the same symmetry in order of increasing energy by integers starting at 1 for the state of lowest energy for a particular symmetry.

The possible electron transitions among the energy levels are determined by the selection rules:

1. $\Delta\Lambda = 0, \pm 1$. The transitions $\Sigma - \Sigma$, $\Pi - \Sigma$, $\Delta - \Pi$, and so forth, are allowed.
2. $\Delta S = 0$. Transitions that change multiplicity are very weak for molecules formed from light atoms, but as spin-orbit coupling increases in heavy atoms, transitions with $\Delta S \neq 0$ become more strongly allowed.
3. $\Delta\Omega = 0, \pm 1$.

Table 1. Angular momenta in diatomic molecules.

Angular Momentum	Projection on Molecular Axis (units of \hbar)
\mathbf{J}	$\Omega = (\Lambda + \Sigma)$
\mathbf{L}	Λ
\mathbf{S}	Σ
\mathbf{R}	—
$\mathbf{N} = \mathbf{R} + \mathbf{L}$	Λ

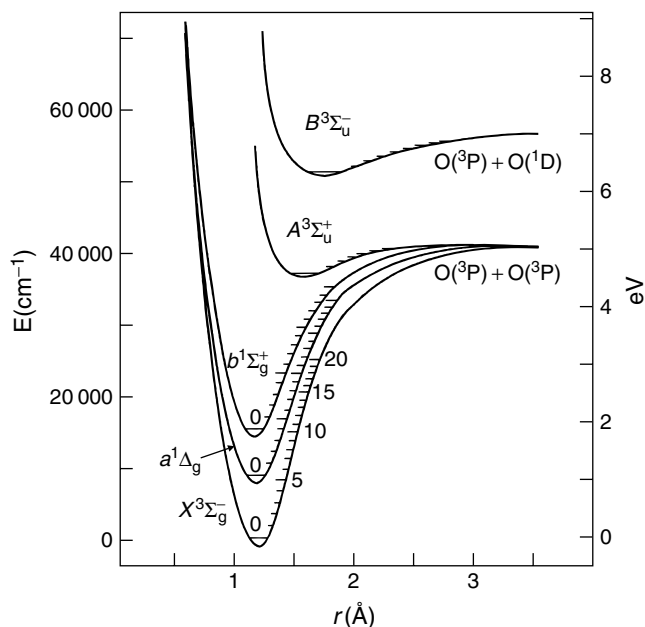


Figure 3. The low-lying electronic states of the O_2 molecule. (From Spectra of Atoms and Molecules by Peter F. Bernath,⁽⁷⁾ copyright 1995 by Oxford University Press, Inc. Used by permission of Oxford University Press, Inc.).

4. $\Sigma^+ - \Sigma^+$, $\Sigma^- - \Sigma^-$, but not $\Sigma^+ - \Sigma^-$. This selection rule is a consequence of the μ_z transition dipole moment having Σ^+ symmetry. Notice that $\Sigma^+ - \Pi$ and $\Sigma^- - \Pi$ transitions are both allowed.
5. $g \leftrightarrow u$. The transitions ${}^1\Pi_g - {}^1\Pi_u$, ${}^1\Sigma_u^+ - {}^1\Sigma_g^+$, and so forth, are allowed for centrosymmetric molecules.

For example, transitions among the first three electronic states of O_2 ($b^1\Sigma_g^+$, $a^1\Delta_g$, and $X^3\Sigma_g^-$ in Figure 3) are forbidden, but the $B^3\Sigma_u^- - X^3\Sigma_g^-$ transition is allowed. The $B - X$ transition of O_2 , called the *Schumann–Runge system*, is responsible for the absorption of UV light for wavelengths less than 200 nm in the earth's atmosphere.

The subscripts g (gerade) and u (ungerade) are only used to classify the electronic states of homonuclear molecules. The electronic wave function is either even (g) or odd (u) with respect to the inversion operation in the molecular frame, that is,

$$\hat{i}\psi_e = \pm\psi_e \quad (28)$$

The superscript + and – signs are attached to Σ states of all diatomics depending on the results of a reflection operation,

$$\hat{\sigma}_v\psi_e = \pm\psi_e \quad (29)$$

All diatomics have an infinite number of planes of symmetry containing the nuclei. For states with $\Lambda > 0$, the +

or – superscripts are redundant because one of the two Λ -components is always + and the other –.

Although both the $b^1\Sigma_g^+ - X^3\Sigma_g^-$ (A-band) and $a^1\Delta_g - X^3\Sigma_g^-$ transitions are forbidden by electric dipole selection rules, they are weakly allowed by a magnetic dipole mechanism.

6 FRANCK–CONDON PRINCIPLE

An electronic transition is made up of vibrational bands, and each band is in turn made of rotational transitions. In condensed media, the rotational structure is generally suppressed although, for example, in superfluid liquid He droplets, nearly free rotation occurs.⁽¹³⁾ The vibrational bands are labeled as $v' - v''$ (single prime denotes upper states and double primes lower states), and an electronic transition is often called a *band system*. The vibrational band positions in an electronic transition are given by

$$\begin{aligned} \tilde{\nu}_{v',v''} = E' - E'' = T_e + \omega'_e \left(v' + \frac{1}{2}\right) - \omega'_e x'_e \left(v' + \frac{1}{2}\right)^2 \\ + \dots - \omega''_e \left(v'' + \frac{1}{2}\right) \\ + \omega''_e x''_e \left(v'' + \frac{1}{2}\right)^2 + \dots \end{aligned} \quad (30)$$

in which T_e is the energy separation between the potential minima of the two electronic states.

The intensities of the bands are determined by three factors: the intrinsic strength of the transition, the populations of the levels involved, and the Franck–Condon factors. The derivation of the quantum-mechanical version of the Franck–Condon principle starts with the transition dipole moment (ignoring rotation),

$$\mathbf{M}_{ev} = \int \psi_{n'v'}^* \boldsymbol{\mu} \psi_{n''v''} d\tau \quad (31)$$

in which $\boldsymbol{\mu}$ is the electric dipole moment operator.

Within the Born–Oppenheimer approximation, the vibrational and electronic parts of the transition moment become

$$\mathbf{M}_{ev} = \int S_{v'}^*(r) \left(\int \psi_{n'}^* \boldsymbol{\mu} \psi_{n''} d\tau_e \right) S_{v''}(r) dr \quad (32)$$

The integral in the center over electronic coordinates is called the *transition dipole moment function* $\mathbf{R}(r)$ and is a parametric function of the internuclear distance r . The function can be expanded about the lower state equilibrium bond length as

$$\mathbf{R}(r) = \mathbf{R}_e + \left. \frac{\partial \mathbf{R}}{\partial r} \right|_{r_e} (r - r_e) + \dots \quad (33)$$

so that substitution of equation (33) into equation (32) leads to

$$\mathbf{M}_{\text{ev}} = \mathbf{R}_e \int S_{v'}^*(r) S_{v''}(r) dr + \frac{\partial \mathbf{R}}{\partial r} \Big|_{r_e} \int S_{v'}^*(r - r_e) S_{v''} dr + \dots \quad (34)$$

Keeping only the first term on the right-hand side of equation (33) leads to the quantum-mechanical Franck–Condon principle for the intensity I of a $v' - v''$ band as

$$I_{v'v''} \propto |\mathbf{R}_e|^2 \times \left| \int S_{v'}^* S_{v''} dr \right|^2 = |\mathbf{R}_e|^2 q_{v'v''} \quad (35)$$

The square of the vibrational overlap integral between the two electronic states, $q_{v'v''}$, is called a *Franck–Condon factor*. There is an implicit J dependence that can be included by using the appropriate $S_v(r)$ solved for a particular J value using equation (13).

7 ROTATIONAL LINE STRENGTHS

For singlet–singlet electronic transitions, rovibronic line intensities are determined by the population of the levels, the Franck–Condon factors and the rotational line strength factor $S_{J'J''}$ (usually called a *Hönl–London factor*). In particular, the total power $P_{J'J''}$ (in W/m^3) emitted by an excited rovibronic state $|nv'J'\rangle$ is

$$P_{J'J''} = \frac{16\pi^3}{3\epsilon_0 c^3} \frac{n_{J'}}{(2J' + 1)} \nu^4 q_{v'v''} |\mathbf{R}_e|^2 S_{J'J''} \quad (36)$$

in which $n_{J'}$ is the excited state population in molecules per m^3 , ν is the transition frequency in Hz, $q_{v'v''}$ is the Franck–Condon factor, \mathbf{R}_e is the electronic transition dipole moment in coulomb meters (Cm) and $S_{J'J''}$ is the dimensionless Hönl–London factor.⁽¹⁴⁾

For allowed one-photon singlet–singlet transitions, there are three cases:

1. $\Delta\Lambda = 0$, $\Lambda'' = \Lambda' = 0$. $^1\Sigma^+ - ^1\Sigma^+$ (or $^1\Sigma^- - ^1\Sigma^-$) transitions have only P and R branches (i.e., $\Delta J = \pm 1$); $^1\Sigma - ^1\Sigma$ transitions are referred to as *parallel transitions*, with the transition dipole moment lying along the z -axis.
2. $\Delta\Lambda = \pm 1$. $^1\Pi - ^1\Sigma^+$, $^1\Pi - ^1\Sigma$, $^1\Delta - ^1\Pi$, and so on, transitions have strong Q branches as well as P and R branches (i.e., $\Delta J = 0, \pm 1$). These transitions have a transition dipole moment perpendicular to the molecular axis, and hence are designated as *perpendicular transitions*.
3. $\Delta\Lambda = 0$, $\Lambda' = \Lambda'' \neq 0$. Transitions such as $^1\Pi - ^1\Pi$, $^1\Delta - ^1\Delta$, and so on, are characterized by weak Q

Table 2. Hönl–London factors.

$\Delta\Lambda = 0$	$S_J^R = \frac{(J'' + 1 + \Lambda'')(J'' + 1 - \Lambda'')}{J'' + 1}$
	$S_J^Q = \frac{(2J'' + 1)\Lambda''^2}{J''(J'' + 1)}$
	$S_J^P = \frac{(J'' + \Lambda'')(J'' - \Lambda'')}{J''}$
$\Delta\Lambda = +1$	$S_J^R = \frac{(J'' + 2 + \Lambda'')(J'' + 1 + \Lambda'')}{4(J'' + 1)}$
	$S_J^Q = \frac{(J'' + 1 + \Lambda'')(J'' - \Lambda'')(2J'' + 1)}{4J''(J'' + 1)}$
	$S_J^P = \frac{(J'' - 1 - \Lambda'')(J'' - \Lambda'')}{4J''}$
$\Delta\Lambda = -1$	$S_J^R = \frac{(J'' + 2 - \Lambda'')(J'' + 1 - \Lambda'')}{4(J'' + 1)}$
	$S_J^Q = \frac{(J'' + 1 - \Lambda'')(J'' + \Lambda'')(2J'' + 1)}{4J''(J'' + 1)}$
	$S_J^P = \frac{(J'' - 1 + \Lambda'')(J'' + \Lambda'')}{4J''}$

branches (for small Λ) and strong P and R branches ($\Delta J = 0, \pm 1$).

The rotational line strength factors⁽⁶⁾ are given in Table 2 for these various cases. Note that for the Hönl–London factors in Table 2, there is an implicit definition of the form of the electronic transition dipole moment because of the separation into electronic, vibrational, and rotational parts. The values in Table 2 assume μ_z and $\mu_x \pm i\mu_y$ are used for the components electronic transition dipole moments in the molecular frame. Note, however, that if the recommended form⁽¹⁶⁾ of $(\mu_x \pm i\mu_y)/\sqrt{2}$ for the perpendicular part is used instead, then the $\Delta\Lambda = \pm 1$ Hönl–London factors in Table 2 need to be multiplied by 2 in order to keep the overall $|\mathbf{M}_{\text{evr}}|^2$ the same.

The line intensities for nonsinglet transitions have to be handled on a case-by-case basis and there are no general formulas.^(11,15,16) Factors for forbidden transitions and multiphoton line strengths also often need to be derived for particular cases, although some of the formulas are available in the literature.⁽¹⁷⁾

8 SPECTROSCOPIC CONSTANTS AND POTENTIAL ENERGY CURVES FROM AB INITIO CALCULATIONS

The primary spectroscopic constants for the electronic states of diatomic molecules are the dissociation energy, D_0 , the equilibrium bond length, r_e , the equilibrium vibrational

frequency, ω_e , and the energy (term value) of the state relative to the ground state, T_e .

Ab initio calculations using a number of widely available computer codes can provide useful estimates of the primary molecular constants. These quantities are most easily calculated for ground states ($T_e = 0$, by definition), by using the analytical first derivative of energy with respect to r to locate the minimum on the potential curve. The harmonic vibrational frequency is then calculated from the second derivative of energy with respect to r , evaluated (numerically or analytically) at r_e . The calculation of dissociation energies is also (in principle) straightforward for a molecule AB, with

$$D_0 = E_A + E_B - E_{AB} - \frac{\omega_e}{2} \quad (37)$$

using total energies and correcting for the zero-point vibrational energy, $\omega_e/2$. The calculation of reliable dissociation energies, however, is relatively difficult because the atoms A and B are sufficiently different in electron distribution from the molecule AB that errors in the calculations of E_A , E_B , and E_{AB} tend not to cancel when the dissociation energy is computed.

More sophisticated calculations of spectroscopic properties are best carried out by computing a number of points on the potential surface, fitting the points to a function, and then solving the one-dimensional Schrödinger equation (equation 13) numerically using a program such as LEVEL [2].⁽¹⁸⁾ The computed rovibrational levels can be fitted with the usual energy level expressions, (17) to (20), to extract the spectroscopic constants, including centrifugal distortion constants, (e.g., D_v) anharmonic vibrational constants (e.g., $\omega_e x_e$) and vibration-rotation interaction constants (e.g., α_e). An equivalent procedure fits the calculated potential points to the Dunham potential (equation 15). Dunham relationships⁽¹⁰⁾ are then used to convert the set of a_i to the corresponding set of spectroscopic Dunham Y_{ij} parameters (see equation 16).

For example, Lee and Dateo⁽¹⁹⁾ calculated the ground state potential energy curve of CN ($X^2\Sigma^+$) and CN^- ($X^1\Sigma^+$) with large augmented correlation-consistent basis sets (up to aug-cc-p-V5Z) and the CC, coupled cluster with single, double and partial triple excitations (CCSD(T)), technique for electron correlation. The comparison of experiment⁽²⁰⁾ and theory for CN (CN^- is unknown) is given in Table 3.

Calculations are now sufficiently reliable (very large basis sets and extensive correlation) that they can be limited by the breakdown of the Born-Oppenheimer approximation. The simplest correction that can be computed is the

Table 3. Comparison of calculated and observed spectroscopic constants for $X^2\Sigma^+$ state of CN (in cm^{-1}).

Constant	'Best' theory ^a	Experiment ^b
$r_e(\text{\AA})$	1.1739	1.17180749(21)
B_0	1.88435	1.89109067(19)
B_e	1.89294	1.89978316(67)
α_e	0.01720	0.0173720(12)
ω_e	2067.7	2068.648(11)
$\omega_e x_e$	12.93	13.097(68)
$\Delta G_{1/2}$	2041.8	2042.41851(68)

^aT.J. Lee and C.E. Dateo (1999) *Spectrochim. Acta A*, **55**, 739.⁽¹⁹⁾

^bC.V.V. Prasad and P.F. Bernath (1992) *J. Mol. Spectrosc.*, **156**, 327.⁽²⁰⁾

'diagonal correction' in equation (7), that is,

$$\Delta E = \langle \psi_n | \hat{T}_N | \psi_n \rangle = -\frac{\hbar^2}{2} \langle \psi_n | \sum_{\alpha} \frac{1}{m_{\alpha}} \nabla_{\alpha}^2 | \psi_n \rangle \quad (38)$$

This is simply the first-order correction of the nuclear kinetic energy operator using the electronic wave function; in this form no additional mass-polarization terms are needed.⁽²¹⁾ When the Born-Oppenheimer separation was made, the electronic Schrödinger equation was derived by neglecting \hat{T}_N . Martin,⁽²²⁾ for example, has found that this diagonal (adiabatic) correction makes a nonnegligible contribution to the calculation of the spectroscopic constants for H_2 , LiH, BeH, and BH. He confirms that atomic masses (not nuclear masses) should be used. Basically, the use of atomic masses compensates for some of the missing non-diagonal (nonadiabatic corrections) for Born-Oppenheimer breakdown.

For H_2 , the nondiagonal corrections have been computed to high accuracy; for example, Wolniewicz⁽²³⁾ has computed the Born-Oppenheimer potential of H_2 using a flexible expansion in elliptical coordinates. The diagonal Born-Oppenheimer corrections to the potential were calculated, and a variation-perturbation method used to compute the nonadiabatic corrections to the vibration-rotation energy levels of H_2 , D_2 , T_2 , HD, HT, and DT. The errors in the energy level differences are believed to be on the order of 0.001 cm^{-1} . Alternative approaches to the calculation of nonadiabatic energies of H_2 include diffusion Monte Carlo^(24,25) and the use of explicitly correlated Gaussian functions.⁽²⁶⁾ These methods are all rather specialized (i.e., suitable for H_2), however, and are not easily generalized to other systems.

Diagonal corrections to the Born-Oppenheimer approximation are relatively easy to compute⁽²²⁾ and they result in a mass-dependent change to the potential curve. Nonadiabatic corrections, however, couple excited $^1\Pi_g$ states to the ground $X^1\Sigma_g^+$ state (in the case of H_2) and this interaction

depends on v and J . Unfortunately, the nonadiabatic corrections are generally comparable in size to the simple diagonal corrections (see Reference 27). Schwenke⁽²⁸⁾ has recently carried out an ab initio implementation of the Bunker and Moss⁽²⁹⁾ formulation of the nonadiabatic corrections. This approach seems to be generally applicable to diatomic and small polyatomic molecules.

The calculation of excited-state potential curves of diatomics is more difficult than for the ground state. Taking differences of orbital energies from a Hartree-Fock self-consistent field, (HF-SCF), calculation is not a suitable or even correct approach. The best simple procedure (which in spite of its name does not include any electron correlation) is called the *configuration interaction singles* (CIS) approach. Excited states are represented by the optimum linear combination of Slater determinants constructed from the singly excited orbitals of the HF ground state (see Reference 30). More realistic calculations, however, need to include electron correlation and the optimization of orbitals to represent excited states better.

The multiconfiguration self-consistent field (MC-SCF) method is a reliable approach to the calculation of low-lying potential energy curves of diatomic molecules (see References 31, 32). The electronic wave function is approximated as a linear combination of Slater determinants, and the orbitals as well as the mixing coefficients of the Slater determinants, are optimized at the same time. A very useful version of the MC-SCF approach is to include all determinants constructed from the ground state by exciting the valence electrons (i.e., valence electrons distributed among the valence orbitals in all possible ways). This complete-active-space self-consistent field (CASSCF) method provides excellent starting wave functions for all of the low-lying valence states. Additional electron correlation can be added by configuration interaction (CI). For

transition metal-containing diatomics, the CASSCF-CI procedure gives good predictions of spectroscopic constants including T_e .

An example of a CASSCF calculation followed by a multireference CI is the work of Langhoff and Bauschlicher⁽³³⁾ on NbN. In this case, they carried out a ‘state averaging’, that is, a single common set of optimized molecular orbitals was used for each multiplicity (singlet, triplet, and quintet). The Nb atom core electrons were not treated explicitly, but their effect was described using a relativistic effective core potential.⁽³⁴⁾ Figure 4 displays the calculated potential curves. All of the low-lying states of NbN are now known,⁽³⁵⁾ and an experimental–theoretical comparison is made in Table 4. The agreement is rather good: $\pm 0.02 \text{ \AA}$

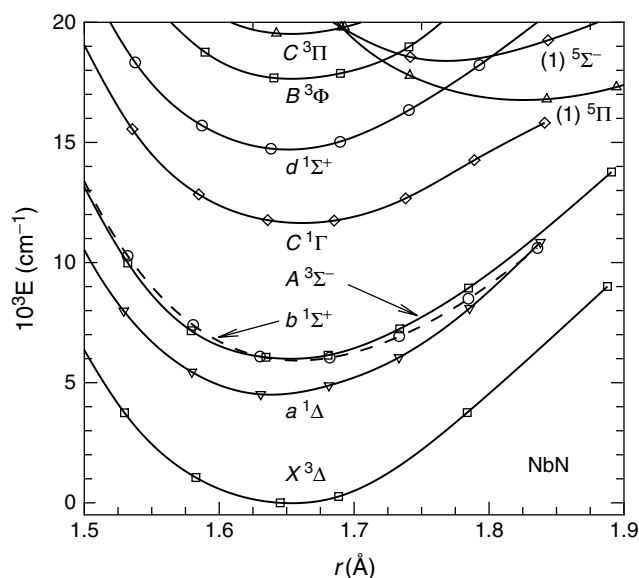


Figure 4. Calculated potential energy curves for the low-lying electronic states of NbN (after S.R. Langhoff and C.W. Bauschlicher (1990) *J. Mol. Spectrosc.*, **143**, 169).⁽³³⁾

Table 4. Comparison of calculated and observed spectroscopic constants for NbN.

State	Theory ^a			Experiment ^b		
	r_e (Å)	ω_e (cm ⁻¹)	T_e (cm ⁻¹)	r_e (Å)	$\Delta G_{1/2}$ (cm ⁻¹)	T_e (cm ⁻¹)
$X^3\Delta$	1.675	1008	0	1.659	1034	0
$A^3\Sigma^-$	1.684	999	4925	1.669	1017	4949
$B^3\Phi$	1.684	946	16 753	1.671 ^c	—	16 518 ^{c,d}
$C^3\Pi$	1.684	934	18 192	1.669	980	17 049
$a^1\Delta$	1.667	932	3999	1.649	1063	4812
$b^1\Sigma^+$	1.683	976	4909	1.663	1017	5454
$c^1\Gamma$	1.682	978	10 201	1.665 ^c	—	9512
$d^1\Sigma^+$	1.674	1057	12 878	1.656	1041	13 511
$e^1\Pi$	1.689	911	18 939	1.672 ^c	—	18 457

^aS.R. Langhoff and C.W. Bauschlicher (1990) *J. Mol. Spectrosc.*, **143**, 169.⁽³³⁾

^bR.S. Ram and P.F. Bernath (2000) *J. Mol. Spectrosc.*, **201**, 267.⁽³⁵⁾

^c r_0 values.

^dY. Azuma, G. Huang, M.P.J. Lyne, A.J. Merer, and V.I. Srdanov (1994) *J. Chem. Phys.*, **100**, 4138.⁽³⁶⁾

for r_e , 50 cm^{-1} for ω_e and 1000 cm^{-1} for T_e , even without explicitly including the effects of spin-orbit coupling.

An alternative approach to excited-state calculations is the equation-of-motion coupled-cluster (EOM-CC) method,⁽³⁰⁾ which is related to propagator methods and multireference CC methods. The EOM-CC method works well for the calculation of properties of excited states (including ionization potentials) of diatomics such as BH, CH⁺ and C₂.⁽³⁷⁾

9 CALCULATION OF RELATIVISTIC EFFECTS

When relativity is considered, several additional terms need to be added to the nonrelativistic electronic Hamiltonian operator. Relativistic effects are all ultimately based on the Dirac equation for a single electron in a potential.⁽³⁸⁾ For multielectron atoms in the absence of external fields, the Breit-Pauli Hamiltonian contains some additional terms including,⁽³⁹⁾

$$\hat{\mathbf{H}}_{\text{mv}} = -\frac{\alpha^2}{8} \sum_{i=1}^N \hat{\mathbf{p}}_i^4 \quad (39)$$

$$\hat{\mathbf{H}}_{\text{d}} = \frac{\alpha^2}{8} \sum_i \nabla_i^2 \hat{\mathbf{V}} \quad (40)$$

$$\hat{\mathbf{H}}_{\text{so}} = \frac{\alpha^2}{2} \left[\sum_i \frac{Z}{r_i^3} \hat{\mathbf{l}}_i \cdot \hat{\mathbf{s}}_i - \sum_{i \neq j} \frac{(\mathbf{r}_{ij} \times \mathbf{p}_i) \cdot (\hat{\mathbf{s}}_i + 2\hat{\mathbf{s}}_j)}{r_{ij}^3} \right] \quad (41)$$

in atomic units with the dimensionless fine-structure constant,

$$\alpha = \frac{\mu_0 e^2 c}{2h} \approx \frac{1}{137} \quad (42)$$

Note that $1/\alpha$ is the speed of light in atomic units. The ‘mass-velocity’ term, $\hat{\mathbf{H}}_{\text{mv}}$, with $\hat{\mathbf{p}}_i = -i\nabla_i$ accounts for the usual relativistic increase in mass of the electron with velocity. This term causes the s-orbitals of atoms to shrink in size because s electrons move rapidly as they get close to the nucleus.⁽⁴⁰⁾ The Darwin term, $\hat{\mathbf{H}}_{\text{d}}$, causes a small shift in the energy levels of an atom. However, the spin-orbit term, $\hat{\mathbf{H}}_{\text{so}}$, is by no means a small correction for heavy atoms, and can be included in the zeroth-order nonrelativistic Hamiltonian.

The effects of mass-velocity, Darwin and spin-orbit terms can be included in a relativistic effective core potential.⁽³⁴⁾ In this case, the ab initio calculations give improved results, even though only the nonrelativistic electronic Schrödinger equation is used for the valence electrons. Neglected additional terms include electron

spin-spin coupling, which is usually dominated by second-order spin-orbit coupling for heavy atoms rather than true spin-spin coupling.

Because the Breit-Pauli Hamiltonian is difficult to use in practical calculations, the Douglas-Kroll transformation of the Dirac equation is often preferred.^(41,42) The spin-orbit part of the Douglas-Kroll Hamiltonian has the same form as equation (41) and the remaining terms (equivalent to mass-velocity and Darwin terms) are responsible for ‘scalar’ relativistic effects. The inclusion of these scalar relativistic effects is necessary, for example, in the calculation of reliable dissociation energies of diatomics such as CF.⁽⁴³⁾

Spin-orbit coupling is generally included in ab initio calculations through the Breit-Pauli spin-orbit operator, $\hat{\mathbf{H}}_{\text{so}}$, equation (41). For molecules, a sum over atoms is needed and $\hat{\mathbf{l}}_i$ is replaced by $\hat{\mathbf{r}}_i \times \hat{\mathbf{p}}_i$ in the first term on the right-hand side. The second term on the right-hand side is the ‘spin-other-orbit’ interaction. Given a set of good wave functions for the electronic states of a diatomic, the first-order energies,

$$E_n^{(1)} = \langle \psi_n | \hat{\mathbf{H}}_{\text{so}} | \psi_n \rangle \quad (43)$$

are readily computed to give the spin-orbit splittings of the spin components $|^{2S+1}\Lambda_\Omega\rangle$ of a given term. Spin-orbit coupling (equation 41) can also couple spin components of different $^{2S+1}\Lambda$ terms, giving

$$E_{mn}^{(1)} = \langle \psi_m | \hat{\mathbf{H}}_{\text{so}} | \psi_n \rangle \quad (44)$$

and in this case a larger matrix of all of the low-lying spin components needs to be diagonalized.

Fleig and Marion⁽⁴⁴⁾ have carried out ab initio calculations on PtH and PtD to predict the spectroscopic properties of the low-lying states. PtH has a $5d^9$ Pt configuration that results in low-lying $^2\Sigma^+$, $^2\Pi_{3/2}$, $^2\Pi_{1/2}$, $^2\Delta_{5/2}$, $^2\Delta_{3/2}$ spin components from the d-hole (i.e., $5d\sigma$, $5d\pi$ and $5d\delta$ states). Wave functions for the spin-free system were derived from a CASSCF-CI calculation. In the second step, diagonal and off-diagonal spin-orbit matrix elements were computed for the five electronic basis functions (two $\Omega = 1/2$, two $\Omega = 3/2$, and one $\Omega = 5/2$). Fleig and Marion also added three additional terms⁽¹¹⁾ to their calculation, namely,

$$\begin{aligned} \hat{\mathbf{H}}_{\text{corr}} = & \frac{1}{2\mu r^2} (\mathbf{L}^+ \mathbf{S}^- + \mathbf{L}^- \mathbf{S}^+) - \frac{1}{2\mu r^2} (\mathbf{J}^+ \mathbf{S}^- + \mathbf{J}^- \mathbf{S}^+) \\ & - \frac{1}{2\mu r^2} (\mathbf{J}^+ \mathbf{L}^- + \mathbf{J}^- \mathbf{L}^+) \end{aligned} \quad (45)$$

to account for spin-electronic, \mathbf{S} -uncoupling and \mathbf{L} -uncoupling interactions, and diagonalized their matrices for each value of the rotational quantum number J . The term values for the calculations are compared with experiment⁽⁴⁵⁾ in Table 5 for e parity.

Table 5. Comparison of Calculated and Experimental Energy Levels of PtD and PtD (in cm^{-1}).

State	PtH Calc. ^a	PtH Obs. ^b	PtD Calc. ^a	PtD Obs. ^b
$v = 0^2\Delta_{5/2}$	0	0	0	0
$v = 0^2\Sigma_{1/2}$	1479	—	1488	—
$v = 1^2\Delta_{5/2}$	2298	2293	1650	1644
$v = 0^2\Pi_{3/2}$	3414	3254	3428	3243
$v = 1^2\Pi_{3/2}$	5452	5429	4897	4804
$v = 0^2\Delta_{3/2}$	11 626	11 608	11 632	11 606
$v = 0^2\Pi_{1/2}$	12 208	—	12 214	—
$v = 1^2\Delta_{3/2}$	13 812	13 832	13 201	13 201

^aT. Fleig and C.M. Marian (1996) *J. Mol. Spectrosc.*, **178**, 1.⁽⁴⁴⁾

^bM.C. McCarthy, R.W. Field, R. Engleman, and P.F. Bernath (1993) *J. Mol. Spectrosc.*, **158**, 208.⁽⁴⁵⁾

10 CALCULATION OF LIFETIMES AND TRANSITION DIPOLE MOMENTS

The radiative properties of allowed electronic transitions are relatively easy to compute from given equations (32) and (34) and reliable wave functions and potential energy curves. For example, Bauschlicher *et al.*⁽⁴⁶⁾ have computed the Einstein A values and radiative lifetimes for various vibrational bands of the $A^6\Sigma^+ - X^6\Sigma^+$ transition of CrH. CrH is of interest in molecular astronomy, in which it appears prominently in the spectra of substellar objects called *brown dwarfs*. Brown dwarfs are cool (1000–2000 K) objects that are smaller than stars but larger than giant planets such as Jupiter.

The properties of the $A^6\Sigma^+$ and $X^6\Sigma^+$ states of CrH were computed using the MCSCF-CI technique using large basis sets and extensive electron correlation. Scalar relativistic effects were included using the Douglas–Kroll approach. The $A-X$ transition dipole moment (Figure 5) was then computed using various ab initio wave functions and the potential energy curves.

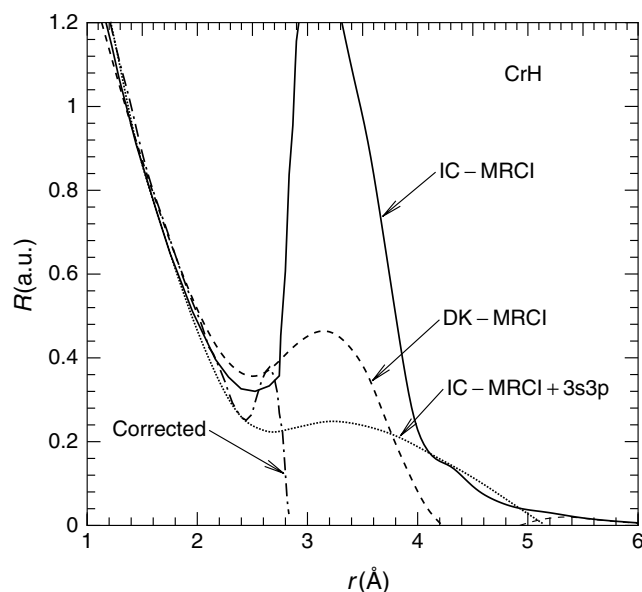


Figure 5. Transition dipole moment as a function of bond distance for the $A^6\Sigma^+ - X^6\Sigma^+$ transition of CrH calculated at various levels of theory [C.W. Bauschlicher, R.S. Ram, P.F. Bernath, C.G. Parsons, and D. Galehouse (2001) *J. Chem. Phys.*, **115**, 1312].⁽⁴⁶⁾

The comparison between experiment and calculation for CrH is given in Table 6. The calculated dissociation energy (2.17 eV) of the ground state is slightly higher than the experimental value (1.93(7) eV) and suggests that there may be a small problem with the experimental value.⁽⁴⁷⁾ The theoretical Einstein A value of the 0–0 band of the $A^6\Sigma^+$ transition is calculated to be 1.20×10^{-6} s with an estimated accuracy of 10%. The various A values can be used to derive the abundance of CrH in brown dwarfs and to model the spectral energy distribution function using molecular opacity functions.

The calculation of transition dipole moments for forbidden transitions is more difficult. The starting point is also a set of good electronic wave functions. The next step is to calculate mixing of the spin components of the relevant

Table 6. Comparison of Experimental and ‘Corrected’ Ab Initio Calculations of Spectroscopic Constants of CrH^a.

Constant	X-state calc.	X-state obs.	A-state calc.	A-state obs.
$r_e(\text{Å})$	1.654	1.655	1.765	1.7865
$D_0(\text{eV})$	2.17	1.93(7)	—	—
$\omega_e(\text{cm}^{-1})$	1653.8	1656.05	1525.2	1524.80
$\omega_e x_e(\text{cm}^{-1})$	31.0	30.49	23.0	22.28
$A_{00}(\text{s}^{-1})$	—	—	1.20×10^{-6}	—

^aC.W. Bauschlicher, R.S. Ram, P.F. Bernath, C.G. Parsons, and D. Galehouse (2001) *J. Chem. Phys.*, **115**, 1312.⁽⁴⁶⁾

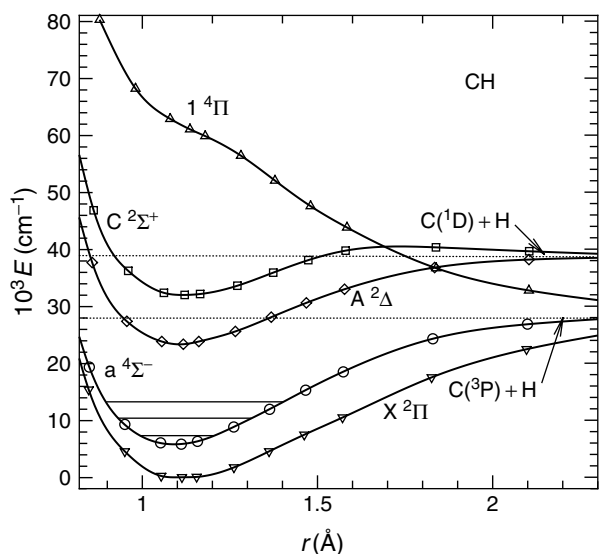


Figure 6. Calculated potential energy curves for the low-lying electronic states of CH [after H. Hettema and D.R. Yarkony, (1994) *J. Chem. Phys.*, **100**, 1998].⁽⁴⁸⁾

electronic states using the Breit–Pauli spin–orbit Hamiltonian (equation 41) using first-order perturbation theory. The transition dipole moment $\mathbf{R}(r)$ can then be computed as for an allowed transition with these mixed wave functions. Rotational interactions can be included, if necessary. Hettema and Yarkony⁽⁴⁸⁾ computed the lifetime of the $a^4\Sigma^-$ state of CH. The relevant potential curves (Figure 6) and wave functions were first computed with the MCSCF-CI approach. The off-diagonal matrix elements of the Breit–Pauli operator were computed for the $a^4\Sigma_{1/2}$, $a^4\Sigma_{3/2}$, $X^2\Pi_{3/2}$ and $X^2\Pi_{1/2}$ spin components of the a and X states. The mixed wave functions were then used to compute the radiative lifetimes of 12, 10, and 8 s for the $v = 0$, 1, and 2 vibrational levels of the $a^4\Sigma^-$ state, using the ab initio potential surface to obtain the needed vibrational wave functions. Einstein A values for individual rovibronic transitions were also computed.

11 CALCULATION OF BOND ENERGIES, IONIZATION POTENTIALS, AND ELECTRON AFFINITIES

The calculation of thermochemical properties is an important application of modern quantum chemistry. The most important quantity is the enthalpy ('heat') of formation ΔH_f° at standard temperature (298.15 K) and pressure (1 bar) of a molecule from its constituent elements in their standard states. For a diatomic molecule, the enthalpy of formation is related to the dissociation energy of the gaseous diatomic AB via

$$D^\circ(\text{AB}) = \Delta H_f^\circ[\text{A}(\text{g})] + \Delta H_f^\circ[\text{B}(\text{g})] - \Delta H_f^\circ[\text{AB}(\text{g})] \quad (46)$$

The heats of formation of the gaseous atomic elements are thus needed to convert dissociation energies into heats of formation. Spectroscopic dissociation energies, D_0 , are effectively 0 K values, however, and need to be converted to 298 K using enthalpy functions (see Committee on Data for Science and Technology (CODATA) values)⁽⁴⁹⁾ although

$$D^\circ(298 \text{ K}) = D_0(0 \text{ K}) + \frac{3}{2}RT \quad (47)$$

is a good approximation.

The calculation of dissociation energies, along with ionization energies and electron affinities, has been the target of several methods such as the G1, G2, G3 (G for Gaussian) series of Pople *et al.*⁽⁵⁰⁾ and the 'complete basis set' (CBS) methods of Petersson *et al.*⁽⁵¹⁾ These methods are based on relatively modest ab initio calculations with several semiempirical corrections added to improve accuracy. They are aimed largely at polyatomic molecules of the first and second rows of the periodic table, but use diatomics as tests. The W1 and W2 (W for Weizmann) schemes of Parthiban and Martin⁽⁵²⁾ use a higher level of theory, and are free of parameters derived from experiment.

For a diatomic, the dissociation energy, ionization energy, and electron affinity are best computed from the appropriate total energies calculated at a high level of theory with as many corrections as possible. The W2 scheme of Martin *et al.*,⁽⁵²⁾ for example, includes geometries at the CCSD(T)/cc-pVQZ+1 level of theory, a correction for basis set incompleteness, a correction for some of the missing correlation energy, a scalar relativistic correction, a spin–orbit correction, and a correction for anharmonicity for the zero-point energies. The W2 theory⁽⁵²⁾ produces heats of formation accurate to 0.23 kcal mol⁻¹, electron affinities to 0.012 eV, and ionization potentials to 0.013 eV for diatomics, and small polyatomics of the first and second rows of the periodic table.

Calculations of thermochemical properties for diatomics containing transition elements, lanthanides, and actinides are more difficult, but the use of relativistic core potentials gives useful values. Indeed, for most diatomics containing heavy elements, experimental values are generally unavailable. A complete set of thermochemical quantities can be computed using statistical mechanics from ab initio total energies, bond lengths, and vibrational frequencies for the low-lying electronic states. The rotational, vibrational, and electronic contributions to the partition functions can be computed from the calculated spectroscopic properties of the electronic states. For example, Jug *et al.*⁽⁵³⁾ computed heat capacities (C_p) and entropies (S) for metal halides. This ab initio approach to thermochemistry is much more reliable than the use of 'estimated' spectroscopic constants

(in, for example, the JANAF tables)⁽⁵⁴⁾ when experimental data is unavailable.

12 CONCLUSION

The ab initio calculation of molecular properties associated with the electronic transitions of diatomic molecules has become an important partner in the interpretation of spectra. Experimental measurements of electronic spectra, particularly for systems containing transition metals, are often incomplete. For example, we have recorded the infrared electronic emission spectra of the new molecules RuN⁽⁵⁵⁾ and OsN.⁽⁵⁶⁾ Transition metal nitrides are of interest in the fixation of nitrogen in industrial, inorganic, and biological systems. Without ab initio calculations of the properties of the low-lying states by Liévin,^(55,56) we would not have been able to interpret our spectra. The calculations demonstrated, for example, that although RuN and OsN are isovalent (Fe, Ru, and Os are in group 8 of the periodic table), RuN has a ground $X^2\Sigma^+$ state, while OsN has a ground $X^2\Delta_{5/2}$ state. Even though ab initio calculations of diatomics have achieved ‘spectroscopic accuracy’ only for systems such as H₂, modern calculations can give a reliable ‘big picture’ for the electronic structure. Such information is an invaluable guide to the interpretation of observed spectra and as a supplement to measurements when no other information is available.

NOTE

- [1] LeRoy, R.J. (2001) *Energies, Intensities and Potentials: Concepts and Tools in Spectroscopy*, unpublished lecture notes.

REFERENCES

- Gaydon, A.G. (1974) *The Spectroscopy of Flames*, 2nd edition, Chapman & Hall, London.
- Rees, M.H. (1989) *Physics and Chemistry of the Upper Atmosphere*, Cambridge University Press, Cambridge.
- Goody, R.M. and Yung, Y.L. (1989) *Atmospheric Radiation: Theoretical Basis*, Oxford University Press, New York.
- Fowler, A. (1904) *Proc. R. Soc. London A*, **73**, 219.
- Born, M. and Oppenheimer, J.R. (1927) *Ann. Phys.-Leipzig*, **84**, 457.
- Herzberg, G. (1950) *Spectra of Diatomic Molecules*, 2nd edition, Van Nostrand Reinhold, New York.
- Bernath, P.F. (1995) *Spectra of Atoms and Molecules*, Oxford University Press, New York.
- Pack, R.T. and Hirschfelder, J.O. (1968) *J. Chem. Phys.*, **49**, 4009.
- Ogilvie, J.F. (1998) *The Vibrational and Rotational Spectrometry of Diatomic Molecules*, Academic Press, San Diego, Calif.
- Dunham, J.L. (1932) *Phys. Rev.*, **41**, 721.
- Lefebvre-Brion, H. and Field, R.W. (1986) *Perturbations in the Spectra of Diatomic Molecules*, Academic Press, Orlando.
- Bunker, P.R. and Jensen, P. (1998) *Molecular Symmetry and Spectroscopy*, 2nd edition, NRC Research Press, Ottawa.
- Grebenev, S., Hatmann, M., Havenith, M., Sartakov, B., Toennies, J.P., and Vilesov, A.F. (2000) *J. Chem. Phys.*, **112**, 4485.
- Whiting, E.E., Schadee, A., Tatum, J.B., Hougen, J.T., and Nicholls, R.W. (1980) *J. Mol. Spectrosc.*, **80**, 249.
- Kovacs, I. (1969) *Rotational Structure in the Spectra of Diatomic Molecules*, Adam Hilger, London.
- Whiting, E.E., Paterson, J.A., Kovacs, I., and Nicholls, R.W. (1973) *J. Mol. Spectrosc.*, **47**, 84.
- Hipler, M. (1999) *Mol. Phys.*, **97**, 105.
- LeRoy, R.J. (2001) LEVEL 7.4, University of Waterloo, ON, Canada, Chemical Physics Report, CP-642; <http://leroy.uwaterloo.ca/>
- Lee, T.J. and Dateo, C.E. (1999) *Spectrochim. Acta A*, **55**, 739.
- Prasad, C.V.V. and Bernath, P.F. (1992) *J. Mol. Spectrosc.*, **156**, 327.
- Kutzelnigg, W. (1997) *Mol. Phys.*, **90**, 909.
- Martin, J.M.L. (1998) *Chem. Phys. Lett.*, **292**, 411.
- Wolniewicz, L. (1995) *J. Chem. Phys.*, **103**, 1792.
- Chen, B. and Anderson, J.B. (1995) *J. Chem. Phys.*, **102**, 2802.
- Anderson, J.B. (1995) in *Quantum Mechanical Electronic Structure Calculations with Chemical Accuracy*, ed. S.R. Langhoff, Kluwer Academic Press, Dordrecht.
- Kinghorn, D.B. and Adamowicz, L. (1999) *Phys. Rev. Lett.*, **83**, 2541.
- Ogilvie, J.F. (1997) *Chem. Phys. Lett.*, **267**, 590.
- Schwenke, D.W. (2001) *J. Phys. Chem. A*, **105**, 2352.
- Bunker, P.R. and Moss, R.E. (1977) *Mol. Phys.*, **33**, 417.
- Bartlett, R.J. and Stanton, J.F. (1994) in *Reviews in Computational Chemistry*, Vol. V, eds K.B. Lipkowitz and D.B. Boyd, VCH, New York.
- Bauschlicher, C.W. and Langhoff, S.R. (1991) *Chem. Rev.*, **91**, 701.
- Partridge, H., Langhoff, S.R., and Bauschlicher, C.W. (1995) in *Quantum Mechanical Electronic Structure Calculations with Chemical Accuracy*, ed. S.R. Langhoff, Kluwer Academic Press, Dordrecht.
- Langhoff, S.R. and Bauschlicher, C.W. (1990) *J. Mol. Spectrosc.*, **143**, 169.
- Krauss, M. and Stevens, W.J. (1984) *Annu. Rev. Phys. Chem.*, **35**, 357.

35. Ram, R.S. and Bernath, P.F. (2000) *J. Mol. Spectrosc.*, **201**, 267.
36. Azuma, Y., Huang, G., Lyne, M.P.J., Merer, A.J., and Srdanov, V.I. (1994) *J. Chem. Phys.*, **100**, 4138.
37. Hirata, S., Nooijen, M., and Bartlett, R.J. (2000) *Chem. Phys. Lett.*, **328**, 459.
38. Bethe, H.A. and Salpeter, E.E. (1957) *Quantum Mechanics of One- and Two-Electron Atoms*, Springer-Verlag, Berlin.
39. Balasubramanian, K. (1997) *Relativistic Effects in Chemistry, Theory and Techniques, Part A*, Wiley & Sons, New York.
40. Christiansen, P.A., Ermler, W.C., and Pitzer, K.S. (1985) *Annu. Rev. Phys. Chem.*, **36**, 407.
41. Hess, B.A. (1986) *Phys. Rev. A*, **33**, 3742.
42. Hess, B.A. (1997) *Ber. Bunsen-Ges. Phys. Chem.*, **101**, 1.
43. Bauschlicher, C.W. (2000) *J. Phys. Chem. A*, **104**, 2281.
44. Fleig, T. and Marian, C.M. (1996) *J. Mol. Spectrosc.*, **178**, 1.
45. McCarthy, M.C., Field, R.W., Engleman, R., and Bernath, P.F. (1993) *J. Mol. Spectrosc.*, **158**, 208.
46. Bauschlicher, C.W., Ram, R.S., Bernath, P.F., Parsons, C.G., and Galehouse, D. (2001) *J. Chem. Phys.*, **115**, 1312.
47. Chen, Y.-M., Clemmer, D.E., and Armentrout, P.B. (1993) *J. Chem. Phys.*, **98**, 4929.
48. Hettema, H. and Yarkony, D.R. (1994) *J. Chem. Phys.*, **100**, 1998.
49. Cox, J.D., Wagman, D.D., and Medvedev, V.A. (1989) *CODATA Key Values for Thermodynamics*, Hemisphere, New York; <http://www.codata.org/>
50. Curtiss, L.A., Raghavachari, K., Redfern, P.D., Rassolov, V., and Pople, J.A. (1998) *J. Chem. Phys.*, **109**, 7764.
51. Montgomery, J.A., Frisch, M.J., Ochterski, J.W., and Petersson, G.A. (1999) *J. Chem. Phys.*, **110**, 2822.
52. Parthiban, S. and Martin, J.M.L. (2001) *J. Chem. Phys.*, **114**, 6014.
53. Jug, K., Janetzko, F., and Köster, A.M. (2001) *J. Chem. Phys.*, **114**, 5472.
54. Chase, M.W. (1998) NIST-JANAF Thermochemical Tables, 4th edition, *J. Phys. Chem. Ref. Data*, Monograph No. 9.
55. Ram, R.S., Liévin, J., and Bernath, P.F. (1998) *J. Chem. Phys.*, **109**, 6329.
56. Ram, R.S., Liévin, J., and Bernath, P.F. (1999) *J. Chem. Phys.*, **111**, 3449.